

Error Inhibiting Methods for Finite Elements

A. Ditkowski

School of Mathematical Sciences, Tel Aviv University, Tel Aviv 69978, Israel

A. Le Blanc

School of Mathematical Sciences, Tel Aviv University, Tel Aviv 69978, Israel

C.W Shu

Division of Applied Mathematics, Brown University, Providence, RI 02912, USA

Abstract

Finite Difference methods (FD) are one of the oldest and simplest methods used for solving differential equations. Theoretical results have been obtained during the last six decades regarding the accuracy, stability and convergence of the FD method for partial differential equations (PDE).

The local truncation error is defined by applying the difference operator to the exact solution u . In the classical FD method, the orders of the global error and the truncation error are the same.

Block Finite Difference methods (BFD) are difference methods in which the domain is divided into blocks, or cells, containing two or more grid points with a different scheme used for each grid point, unlike the standard FD method. In this approach, the interaction between the different truncation errors and the dynamics of the scheme may prevent the error from growing, hence error reduction is obtained. The phenomenon in which the order of the global error is smaller than the one of the truncation error is called *error inhibition*, see e.g.[8].

The Finite Element method (FE) consists in finding an approximation of the solution in a certain form, usually a linear combination of a set of chosen trial functions, i.e. $\sum q_j \varphi_j$. Since, in most cases, the exact solution will not lie in the space spanned by those functions, the coefficients of the

Email addresses: `adid@tauex.tau.ac.il` (A. Ditkowski), `anneleb@mail.tau.ac.il` (A. Le Blanc), `chi-wang_shu@brown.edu` (C.W Shu)

linear combination can be chosen in such a way that the numerical solution approximates the PDE in a given sense. The Discontinuous Galerkin (DG) method is a class of Finite Element (FE) method using a completely discontinuous polynomial space for the approximation of the solution and trial functions.

It is worth noting that the structure of the BFD method is similar to the structure of the DG method as far as the linear algebraic system to be solved is concerned. In this method as well, the phenomenon of error inhibition may be observed [19].

We first show that our BFD scheme can be viewed as a DG scheme, proving stability during the process. Then, performing a Fourier like analysis, we prove optimal convergence of the BFD scheme.

Keywords: Finite Difference, Block Finite Difference, Finite Elements, Discontinuous Galerkin

1. Introduction

Consider the following differential problem:

$$\begin{cases} \frac{\partial u}{\partial t} = P \left(\frac{\partial}{\partial x} \right) u, & x \in R^d, t \geq 0 \\ u(t=0) = f(x) \end{cases} \quad (1)$$

where $u = (u_1, u_2, \dots, u_m)$ and $P \left(\frac{\partial}{\partial x} \right)$ is a linear differential operator with appropriate boundary conditions. It is assumed that the problem is well-posed, meaning there exists $\kappa(t) < \infty$ such that $\|u(t)\| < \kappa(t)\|f\|$ where typically $\kappa(t) = \kappa e^{\alpha t}$.

Definition 1 (Discrete Norm). $(\cdot, \cdot)_h$ is the discrete norm defined as follows:

$$(u, v)_h = h \sum_j \bar{u}_j v_j$$

where $h = \max_L h_L$ and h_L are the grid spaces.

Definition 2 (Scalar Product). We define the equivalent scalar product by

$$(u, v)_H \doteq (u, Hv)_h$$

where H is a Hermitian positive matrix.

Definition 3 (Semibounded Operator). *The operator Q is called semibounded in the H norm if there is a constant α such that $(Qv, v)_H + (v, Qv)_H \leq 2\alpha \|v\|_H^2$.*

Definition 4 (Norm Equivalence). *Assume that there is a constant $K > 0$ and a positive Hermitian matrix H such that*

$$K^{-1}I \leq H \leq KI \quad (2)$$

where I is the unit matrix.

Then the H norm defined by the scalar product $(\cdot, \cdot)_H$ is equivalent to the L_2 norm in the sense that:

$$K^{-1}(v, v) \leq (v, v)_H \leq K(v, v) \quad (3)$$

Let Q be the semi-discretization operator of $P\left(\frac{\partial}{\partial x}\right)$.

We assume the following:

- The discrete operator Q is based on the grid points $\{x_j\}$, $j = 1, \dots, N$.
- Q is semibounded in the above-defined scalar product where H verifies Def. 4.

Definition 5 (Local Truncation Error). *The local truncation error vector, whose j -th entry is defined as follows:*

$$(\mathbf{T}_e)_j \doteq P(w(x_j)) - (Q\mathbf{w})_j$$

where $w(x)$ is a smooth function and \mathbf{w} is the projection of $w(x)$ onto the grid.

It is assumed that the semi-discrete approximation converges in the sense that

$$\lim_{N \rightarrow \infty} \|\mathbf{T}_e\|_H = 0.$$

We consider the semi-discrete approximation :

$$\begin{cases} \frac{\partial \mathbf{v}}{\partial t} = Q\mathbf{v} , t \geq 0 \\ \mathbf{v}(t=0) = f(x) \end{cases} \quad (4)$$

Definition 6 (Global Error). *Let \mathbf{u} be the projection of $u(x, t)$ onto the grid. Then the Global Error is defined by:*

$$\mathbf{E} = \mathbf{u} - \mathbf{v}.$$

We now derive an upper bound on the global error in the H norm. In order to do so, we use the following lemma.

Lemma 1. *As proved in [10, p. 142], let α be a constant, $\beta(t)$ a bounded function, and $u(t) \in C^1(t)$ a function satisfying :*

$$\frac{\partial u}{\partial t} \leq \alpha u(t) + \beta(t) \text{ for } t \geq t_0$$

Then:

$$\begin{aligned} |u(t)| &\leq e^{\alpha(t-t_0)}|u(t_0)| + \int_{t_0}^t e^{\alpha(t-\tau)}|\beta(\tau)|d\tau \\ &\leq e^{\alpha(t-t_0)}|u(t_0)| + \varphi^*(\alpha, t - t_0) \max_{t_0 \leq \tau \leq t} |\beta(\tau)| \end{aligned} \quad (5)$$

where

$$\varphi^*(\alpha, t) = \begin{cases} \frac{1}{\alpha} (e^{\alpha t} - 1) & \text{if } \alpha \neq 0 \\ t & \text{if } \alpha = 0 \end{cases} \quad (6)$$

Using the definition of \mathbf{T}_e , we may state that:

$$\frac{\partial \mathbf{u}}{\partial t} = Q\mathbf{u} + \mathbf{T}_e \quad (7)$$

Then, by subtracting (4) from (7) we obtain:

$$\frac{\partial \mathbf{E}}{\partial t} = Q\mathbf{E} + \mathbf{T}_e \quad (8)$$

Next, by taking the H scalar product with \mathbf{E} , using the semiboundedness of Q and Cauchy-Schwarz inequality the following estimate is obtained:

$$\begin{aligned} \left(\mathbf{E}, \frac{\partial \mathbf{E}}{\partial t} \right)_H &= \frac{1}{2} \frac{\partial}{\partial t} (\mathbf{E}, \mathbf{E})_H = \|\mathbf{E}\|_H \frac{\partial}{\partial t} \|\mathbf{E}\|_H \\ &= (\mathbf{E}, Q\mathbf{E})_H + (\mathbf{E}, \mathbf{T}_e)_H \\ &\leq \alpha (\mathbf{E}, \mathbf{E})_H + \|\mathbf{E}\|_H \|\mathbf{T}_e\|_H . \end{aligned}$$

Thus

$$\frac{\partial}{\partial t} \|\mathbf{E}\|_H \leq \alpha \|\mathbf{E}\|_H + \|\mathbf{T}_e\|_H . \quad (9)$$

where α is the constant derived from the semiboundedness of Q .

Then, applying Lemma 1 to the error in the H norm $\|\mathbf{E}(t)\|_H$, we conclude that:

$$\|\mathbf{E}(t)\|_H \leq e^{\alpha t} \|\mathbf{E}(0)\|_H + \frac{e^{\alpha t} - 1}{\alpha} \max_{0 \leq \tau \leq t} \|\mathbf{T}_e\|_H \quad (10)$$

Eq.(10) states that if the scheme is stable, it converges as well (this is the first part of Lax-Richtmyer well-known theorem [14]). This inequality implies that the global error is at most of the local truncation error order. Indeed, in all standard schemes the global error is of the same order as the truncation error.

Hence, we can ask ourselves whether a better upper bound can be obtained. Therefore, we will not use this non-optimal inequality but rather the expression of the error in terms of the solution operator, using Duhamel's principle (see [10, p. 147]).

1.1. Error Analysis

In this section, we will try and get an explicit expression of the error.

Let us recall that:

$$\frac{\partial \mathbf{E}}{\partial t} = Q\mathbf{E} + \mathbf{T}_e \quad (11)$$

When applying Theorem 4.7.1 [Duhamel's Principle] from [10, p. 147] to \mathbf{E} , we write:

$$\mathbf{E}(t) = S(t, 0)\mathbf{E}(0) + \int_0^t S(t, \tau)\mathbf{T}_e(\tau) d\tau \quad (12)$$

where $S(t, \nu)$ is the homogeneous equation solution operator, such that $\mathbf{v}(t) = S(t, \nu)\mathbf{v}(\nu)$ where $\mathbf{v}(t)$ is the solution of the equation:

$$\frac{\partial \mathbf{v}}{\partial t} = Q\mathbf{v} \quad (13)$$

In order to demonstrate the method, we choose the case where Q is a constant matrix, therefore:

$$S(t, \nu) = e^{(t-\nu)Q}\mathbf{E}(\nu).$$

We can assume that $\mathbf{E}(0)$ is small, e.g. in the order of machine accuracy.

It can be seen from (12) that the global error is governed by $S(t, \tau)\mathbf{T}_e(\tau)$, not only by $\mathbf{T}_e(\tau)$. Therefore, the global error norm $\|\mathbf{E}\|_H$ may be smaller than the local error $\|\mathbf{T}_e\|_H$ if $\|S(t, \tau)\mathbf{T}_e(\tau)\|_H \ll \|\mathbf{T}_e(\tau)\|_H$. The next subsection will present one BFD scheme which utilizes this observation.

2. Block Finite Difference schemes

In this section we present a BFD scheme for the heat equation with periodic boundary conditions,

$$\begin{aligned} \frac{\partial u}{\partial t} &= \frac{\partial^2 u}{\partial x^2}, \quad x \in (0, 2\pi), \quad t \geq 0 \\ u(x, t=0) &= f(x) \end{aligned} \quad (14)$$

2.1. Description of Two Points Block, 5th order scheme

Let us consider the following grid:

$$x_{j-1/4} = x_j - h/4, \quad x_{j+1/4} = x_j + h/4, \quad h = 2\pi/N, \quad j = 1, \dots, N \quad (15)$$

where

$$x_j = h(j-1) + \frac{h}{2} \quad (16)$$

Altogether there are $2N$ points on the grid, with a distance of $h/2$ between them.

We consider the following approximation:

$$\begin{aligned}
\frac{d^2}{dx^2} u_{j-1/4} &\approx \frac{1}{12(h/2)^2} \left[\left(-u_{j-\frac{5}{4}} + 16u_{j-\frac{3}{4}} - 30u_{j-\frac{1}{4}} + 16u_{j+\frac{1}{4}} - u_{j+\frac{3}{4}} \right) + \right. \\
&\quad \left. c \left(u_{j-\frac{5}{4}} - 5u_{j-\frac{3}{4}} + 10u_{j-\frac{1}{4}} - 10u_{j+\frac{1}{4}} + 5u_{j+\frac{3}{4}} - u_{j+\frac{5}{4}} \right) \right] \\
\frac{d^2}{dx^2} u_{j+1/4} &\approx \frac{1}{12(h/2)^2} \left[\left(-u_{j-\frac{3}{4}} + 16u_{j-\frac{1}{4}} - 30u_{j+\frac{1}{4}} + 16u_{j+\frac{3}{4}} - u_{j+\frac{5}{4}} \right) - \right. \\
&\quad \left. c \left(u_{j-\frac{5}{4}} - 5u_{j-\frac{3}{4}} + 10u_{j-\frac{1}{4}} - 10u_{j+\frac{1}{4}} + 5u_{j+\frac{3}{4}} - u_{j+\frac{5}{4}} \right) \right] \quad (17)
\end{aligned}$$

Equivalently:

$$\begin{aligned}
\mathbf{u}_{xx} &\approx \frac{1}{12(h/2)^2} \left[\begin{pmatrix} \ddots & \ddots & \ddots & \ddots & \ddots & \ddots & \ddots \\ & -1 & 16 & -\mathbf{30} & 16 & -1 & \\ & & -1 & 16 & -\mathbf{30} & 16 & -1 \\ & & & \ddots & \ddots & \ddots & \ddots \end{pmatrix} \right. \\
&\quad \left. + c \begin{pmatrix} \ddots & \ddots & \ddots & \ddots & \ddots & \ddots & \ddots \\ & 1 & -5 & \mathbf{10} & -10 & 5 & -1 \\ & -1 & 5 & -10 & \mathbf{10} & -5 & 1 \\ & & \ddots & \ddots & \ddots & \ddots & \ddots \end{pmatrix} \right] \mathbf{u} \quad (18)
\end{aligned}$$

The structure of this scheme, and a similar scheme with first-order truncation error and third-order convergence rate (4th order with post-processing) was assumed in [7],[9]. Further details on the derivation of the scheme are provided in Appendix C.

2.2. Proof of Stability

2.2.1. Motivation

In this section, our goal is to utilize the FE methodology for proving the stability of the BFD scheme. In [7] and [9], the stability was proven using a Fourier-like analysis. The FE stability analysis, however, is more flexible and has the potential to be applicable in situations where the Fourier analysis cannot be used.

2.2.2. The DG Scheme

Discontinuous Galerkin methods ([19]) are a class of finite element methods using completely discontinuous basis functions, usually chosen as piecewise polynomials. Consider the following heat problem

$$\begin{cases} \frac{\partial u}{\partial t} = \frac{\partial^2}{\partial x^2} u, & x \in (0, 2\pi), \quad t \geq 0 \\ u(x, 0) = f(x) \end{cases} \quad (19)$$

We assume the following mesh to cover the computational domain $[0, 2\pi]$, consisting of cells

$$I_j = [x_{j-1/2}, x_{j+1/2}] \text{ for } j = 1, \dots, N, \text{ where}$$

$$0 = x_{1/2} < x_{3/2} < \dots < x_{N+1/2} = 2\pi.$$

The center of each cell is located at $x_j = \frac{1}{2}(x_{j-1/2} + x_{j+1/2})$ and the size of each cell is $\Delta x_j = x_{j+1/2} - x_{j-1/2}$. A uniform mesh is considered here, hence $h = \Delta x = \frac{2\pi}{N}$.

After multiplying the two sides of the equation by a test function, v , and integrating by parts over each cell I_j , we get the following weak formulation of the problem:

$$\int_{I_j} u_t v dx + \int_{I_j} u_x v_x dx - u_x(x_{j+1/2}, t) v(x_{j+1/2}) + u_x(x_{j-1/2}, t) v(x_{j-1/2}) = 0 \quad (20)$$

The next step of the method is to replace the functions u and v by piecewise polynomials of degree at most k .

Since both functions are now discontinuous at all points $x_{j\pm 1/2}$, there is a need to introduce a cleverly chosen numerical flux in order to stabilize the scheme, i.e. replacing the boundary terms $u(x_{j\pm 1/2}, t)$ by single-valued fluxes $\hat{u}_{j\pm 1/2} = \hat{u}(u_{j\pm 1/2}^-, u_{j\pm 1/2}^+)$ and replacing the test function v at the boundaries by the values taken inside the cell. Here, unlike the hyperbolic case, there is no preferred flux direction, therefore we choose a symmetric flux:

$$\begin{aligned} \hat{u}_{x, j+\frac{1}{2}} &= \frac{1}{2} \left[(u_x)_{j+\frac{1}{2}}^- + (u_x)_{j+\frac{1}{2}}^+ \right] \\ \hat{u}_{x, j-\frac{1}{2}} &= \frac{1}{2} \left[(u_x)_{j-\frac{1}{2}}^- + (u_x)_{j-\frac{1}{2}}^+ \right] \end{aligned} \quad (21)$$

Finally, in order to stabilize the scheme, it is necessary to add penalty terms to inter-element boundaries (e.g. adding a Baumann-Oden penalty term, see [3] for more details).

The discontinuous Galerkin scheme is defined as follows: Find $u, v \in V_{\Delta x}$ (where $V_{\Delta x} = \{v : v \text{ is a polynomial of degree at most } k \text{ for } x \in I_j, j = 1, \dots, N\}$) such that:

$$\begin{aligned} \int_{I_j} u_t v dx + \int_{I_j} u_x v_x dx - \hat{u}_x(x_{j+1/2}, t) v^-(x_{j+1/2}) + \hat{u}_x(x_{j-1/2}, t) v^+(x_{j-1/2}) \\ - \frac{1}{2} v_x^-(x_{j+1/2}) \left[u_{j+1/2}^+ - u_{j+1/2}^- \right] - \frac{1}{2} v_x^+(x_{j-1/2}) \left[u_{j-1/2}^+ - u_{j-1/2}^- \right] = 0 \end{aligned} \quad (22)$$

This scheme has been proven to be consistent, stable and of k order accuracy for even k and $k + 1$ for odd k ([19] [2]).

Following [19], we now look at the nodal presentation of the scheme, namely, we present the functions $u(x)$ and $v(x)$, at some nodes. When a linear element basis is used on equidistant grid, $x_{j-1/4}$ and $x_{j+1/4}$, $u(x)$ and $v(x)$ have the form

$$\begin{aligned} u(x) &= u_{j-1/4} \varphi_{j-1/4} + u_{j+1/4} \varphi_{j+1/4} \\ v(x) &= v_{j-1/4} \varphi_{j-1/4} + v_{j+1/4} \varphi_{j+1/4} \end{aligned} \quad (23)$$

where

$$\begin{aligned} \varphi_{j-1/4} &= -\frac{2}{h}(x - x_{j+\frac{1}{4}}) \\ \varphi_{j+1/4} &= \frac{2}{h}(x - x_{j-\frac{1}{4}}) \end{aligned} \quad (24)$$

Collecting the coefficients of $v_{j-1/4}$ and $v_{j+1/4}$ yields the equation for $u_{j-1/4}$ and $u_{j+1/4}$

$$\begin{bmatrix} u_{j-1/4} \\ u_{j+1/4} \end{bmatrix}_t = \left(A \begin{bmatrix} u_{j-5/4} \\ u_{j-3/4} \end{bmatrix} + B \begin{bmatrix} u_{j-1/4} \\ u_{j+1/4} \end{bmatrix} + C \begin{bmatrix} u_{j+3/4} \\ u_{j+5/4} \end{bmatrix} \right) \quad (25)$$

where

$$\begin{aligned} A &= \frac{1}{4h^2} \begin{bmatrix} 7 & -1 \\ 1 & -7 \end{bmatrix} \\ B &= \frac{1}{2h^2} \begin{bmatrix} -12 & 12 \\ 12 & -12 \end{bmatrix} \\ C &= \frac{1}{4h^2} \begin{bmatrix} -7 & 1 \\ -1 & 7 \end{bmatrix} \end{aligned} \quad (26)$$

Clearly, we can write the BFD scheme as defined in Section 2.1 in a similar form, by assembling the matrices A , B , and C as follows:

$$\begin{aligned}
A &= \frac{1}{3h^2} \begin{bmatrix} -1+c & 16-5c \\ -c & -1+5c \end{bmatrix} \\
B &= \frac{1}{3h^2} \begin{bmatrix} -30+10c & 16-10c \\ 16-10c & -30-10c \end{bmatrix} \\
C &= \frac{1}{3h^2} \begin{bmatrix} -1+5c & -c \\ 16-5c & -1+c \end{bmatrix}
\end{aligned} \tag{27}$$

Hence, our goal is to find the corresponding weak formulation of the problem including the Baumann-Oden, and possibly other, penalty terms as well as numerical fluxes, such that our BFD scheme can be viewed as a form of DG scheme.

As done in [19], we choose a linear element basis (23) for the test and trial functions. By replacing in Eq. (22) the fluxes and standard Baumann-Oden penalties by fluxes and penalties with general coefficients, we obtain the following equation:

$$\begin{aligned}
& \int_{x_{j-1/2}}^{x_{j+1/2}} [\varphi_{j-1/4}(u_{j-1/4})_t + \varphi_{j+1/4}(u_{j+1/4})_t] v(x) dx = \\
& - \int_{x_{j-1/2}}^{x_{j+1/2}} [u_{j-1/4}(\varphi_{j-1/4})_x + u_{j+1/4}(\varphi_{j+1/4})_x] v_x(x) dx \\
& + \left[C_1(u)_{j+1/2}^+ + C_2(u)_{j+1/2}^- + C_3(u_x)_{j+1/2}^- + C_4(u_x)_{j+1/2}^+ \right] v_{j+1/2}^- \\
& + \left[D_1(u)_{j-1/2}^+ + D_2(u)_{j-1/2}^- + D_3(u_x)_{j-1/2}^- + D_4(u_x)_{j-1/2}^+ \right] v_{j-1/2}^+ \\
& + (v_x)_{j+1/2}^- \left[E_1(u)_{j+1/2}^+ + E_2(u)_{j+1/2}^- + E_3(u_x)_{j+1/2}^- + E_4(u_x)_{j+1/2}^+ \right] \\
& + (v_x)_{j-1/2}^+ \left[F_1(u)_{j-1/2}^+ + F_2(u)_{j-1/2}^- + F_3(u_x)_{j-1/2}^- + F_4(u_x)_{j-1/2}^+ \right]
\end{aligned} \tag{28}$$

where

$$\begin{aligned}
(u)_{j+1/2}^+ &= u_{j+3/4}\varphi_{j+3/4}(x_{j+1/2}) + u_{j+5/4}\varphi_{j+5/4}(x_{j+1/2}) \\
(u)_{j+1/2}^- &= u_{j-1/4}\varphi_{j-1/4}(x_{j+1/2}) + u_{j+1/4}\varphi_{j+1/4}(x_{j+1/2}) \\
(u)_{j-1/2}^+ &= u_{j-1/4}\varphi_{j-1/4}(x_{j-1/2}) + u_{j+1/4}\varphi_{j+1/4}(x_{j-1/2}) \\
(u)_{j-1/2}^- &= u_{j-5/4}\varphi_{j-5/4}(x_{j-1/2}) + u_{j-3/4}\varphi_{j-3/4}(x_{j-1/2}) \\
&\text{and} \\
(u_x)_{j+1/2}^+ &= u_{j+3/4}\varphi'_{j+3/4}(x_{j+1/2}) + u_{j+5/4}\varphi'_{j+5/4}(x_{j+1/2}) \\
(u_x)_{j+1/2}^- &= u_{j-1/4}\varphi'_{j-1/4}(x_{j+1/2}) + u_{j+1/4}\varphi'_{j+1/4}(x_{j+1/2}) \\
(u_x)_{j-1/2}^+ &= u_{j-1/4}\varphi'_{j-1/4}(x_{j-1/2}) + u_{j+1/4}\varphi'_{j+1/4}(x_{j-1/2}) \\
(u_x)_{j-1/2}^- &= u_{j-5/4}\varphi'_{j-5/4}(x_{j-1/2}) + u_{j-3/4}\varphi'_{j-3/4}(x_{j-1/2})
\end{aligned} \tag{29}$$

Replacing $v(x)$ by $\varphi_{j+1/4}$ and then $\varphi_{j-1/4}$ and comparing with Eq. (27), we obtain a system of 12 equations for 16 unknowns. In order to avoid having unknowns depending on the parameter h , we performed the following scaling:

$$\begin{aligned}
C_1 &= \frac{C_1}{h}, & C_2 &= \frac{C_2}{h}, & D_1 &= \frac{D_1}{h}, & D_2 &= \frac{D_2}{h}, \\
E_3 &= hE_3, & E_4 &= hE_4, & F_3 &= hF_3, & F_4 &= hF_4
\end{aligned} \tag{30}$$

And obtain the following solution:

$$\begin{aligned}
C_1 &= \frac{7}{3}, & C_4 &= \frac{1}{2}, \\
D_1 &= -C_2 - \frac{14}{3}, & D_2 &= \frac{7}{3}, \\
D_3 &= -\frac{1}{2}, & D_4 &= -C_2 - C_3 - \frac{7}{3}, \\
E_1 &= \frac{1}{18}(-8c - 5), & E_4 &= \frac{1}{18}(-c - 1), \\
F_1 &= -C_2 - E_2 - \frac{7}{3}, & F_2 &= \frac{1}{18}(8c + 5) \\
F_3 &= \frac{1}{18}(-c - 1), & F_4 &= \frac{1}{9}(5c - 9C_2 - 9C_3 - 9E_2 - 9E_3 - 13)
\end{aligned} \tag{31}$$

This leaves us with four remaining unknowns to be identified, namely C_2, C_3, E_2, E_3 . In order to determine those, we demand that the scheme is stable. In particular, we use the methodology developed in ([16]) for proving the stability of FE methods. For this purpose, we first define the following operators:

Definition 7 (operators H and $\theta_{j-1/2}$). *The following operator includes the net contribution viewed as the difference between penalties from each side of the left border of the cell I_j , at node $x_{j-1/2}$ in addition to the numerical flux applied to the same node. At the node $x_{j-1/2}$:*

$$H_{j-1/2}^+ = \left[D_1(u)_{j-1/2}^+ + D_2(u)_{j-1/2}^- + D_3(u_x)_{j-1/2}^- + D_4(u_x)_{j-1/2}^+ \right] u_{j-1/2}^+ + (u_x)_{j-1/2}^+ \left[F_1(u)_{j-1/2}^+ + F_2(u)_{j-1/2}^- + F_3(u_x)_{j-1/2}^- + F_4(u_x)_{j-1/2}^+ \right] \quad (32)$$

$$H_{j-1/2}^- = \left[C_1(u)_{j-1/2}^+ + C_2(u)_{j-1/2}^- + C_3(u_x)_{j-1/2}^- + C_4(u_x)_{j-1/2}^+ \right] u_{j-1/2}^- + (u_x)_{j-1/2}^- \left[E_1(u)_{j-1/2}^+ + E_2(u)_{j-1/2}^- + E_3(u_x)_{j-1/2}^- + E_4(u_x)_{j-1/2}^+ \right] \quad (33)$$

and

$$\theta_{j-1/2} = H_{j-1/2}^- - H_{j-1/2}^+ \quad (34)$$

Note that the analysis can be performed at node $j + 1/2$ as well.

The next step consists of adding the contribution from the internal integrals (in terms of the average from the left and right side).

Definition 8 (operator $\Theta_{j-1/2}$). *The following operator includes the average of the contribution in terms of the integrals from each side of the left border of the cell I_j , at node $x_{j-1/2}$, in addition to the previous operator.*

$$\Theta_{j-1/2} = \theta_{j-1/2} + \frac{1}{2} \int_{x_{j-3/2}}^{x_{j-1/2}} (u_x)_{j-1}^2 dx + \frac{1}{2} \int_{x_{j-1/2}}^{x_{j+1/2}} (u_x)_j^2 dx \quad (35)$$

Note that $\Theta_{j-1/2}$ is the total energy which is generated or dissipated per unit time at the interface $x_{j-1/2}$.

Assuming stability is equivalent to proving that the operator $\Theta_{j-1/2}$ is non-positive definite. Its equivalent quadratic form is as follows:

$$\Theta_{j-1/2} = \begin{bmatrix} u_{j-5/4} \\ u_{j-3/4} \\ u_{j-1/4} \\ u_{j+1/4} \end{bmatrix}^T M \begin{bmatrix} u_{j-5/4} \\ u_{j-3/4} \\ u_{j-1/4} \\ u_{j+1/4} \end{bmatrix} \quad (36)$$

where:

$$M = \frac{1}{12h}$$

$$\begin{bmatrix} 8c-31 & \frac{1}{3}(143-40c) & \frac{1}{2}(40c-3(5C_2+4C_3+20E_2+16E_3-7)) & \frac{1}{6}(-88c+135C_2+108C_3+180E_2+144E_3+167) \\ M_{12} & \frac{1}{3}(56c-277) & \frac{1}{2}(-40c+21C_2+12C_3+84E_2+48E_3-19) & \frac{1}{6}(88c-189C_2-108C_3-252E_2-144E_3-257) \\ M_{13} & M_{32} & \frac{1}{3}(-80c+9C_2+36C_3+36E_2+144E_3+10) & \frac{1}{3}(80c-27C_2-72C_3-72E_2-144E_3+74) \\ M_{14} & M_{24} & M_{34} & \frac{1}{3}(-80c+81C_2+2(54C_3+54E_2+72E_3+5)) \end{bmatrix}$$

M is a symmetric singular matrix, therefore we can assume that the fourth row is linearly dependent on the three others, obtaining a first constraint for the unknowns C_2, C_3, E_2, E_3 . Therefore, it is sufficient to assure the non positiveness for the truncated matrix:

$$M' = \frac{1}{12h} \begin{bmatrix} 8c-31 & \frac{1}{3}(143-40c) & \frac{1}{2}(40c-3(5C_2+4C_3+20E_2+16E_3-7)) \\ M_{12} & \frac{1}{3}(56c-277) & \frac{1}{2}(-40c+21C_2+12C_3+84E_2+48E_3-19) \\ M_{13} & M_{32} & \frac{1}{3}(-80c+9C_2+36C_3+36E_2+144E_3+10) \end{bmatrix}$$

Using Sylvester's law of inertia [18], stating that the number of eigenvalues of each sign is an invariant of the associated quadratic form, we perform a similarity transformation on M' , thus obtaining a non-singular matrix S such that $D = SM'S^T$.

One possible solution for the unknowns is $C_2 = -7, C_3 = \frac{25}{6}, E_2 = \frac{1}{18}(8c+89), E_3 = \frac{21(c-27)}{126}$. Equivalently:

$$D = \frac{1}{12h} \begin{bmatrix} 8c-31 & 0 & 0 \\ 0 & \frac{1}{9}(-32)(8c-31)(c(8c+13)-166) & 0 \\ 0 & 0 & D_{33} \end{bmatrix}$$

where

$$\begin{aligned} D_{33} &= -(4096/81)(-31+8c)(-166+13c+8c^2)^2 \\ &\quad (-357523+276776c-71424c^2+6144c^3) \end{aligned} \quad (37)$$

It can be verified that for all values of c between -1 and 1 , the values on the diagonal of S are negative, along with M determinant being zero as required.

2.2.3. Conclusion

In the previous sections, we proved that our Two Points Block 5th order scheme can be viewed as a type of DG scheme. We also showed that the

stability of this scheme can be proved using the tools developed for DG methods.

In the following section, we generalize the principles developed above, for a scheme approximating non periodic problems.

2.3. Generalization to non periodic boundary conditions

Consider the following Dirichlet initial boundary value problem:

$$\begin{cases} \frac{\partial u}{\partial t} = \frac{\partial^2}{\partial x^2} u + F(x, t), & x \in (0, \pi), \quad t \geq 0 \\ u(t=0) = f(x) \\ u(0, t) = g_0(t) \\ u(\pi, t) = g_\pi(t) \end{cases} \quad (38)$$

2.3.1. Adapting the BFD scheme to non periodic boundary conditions of Dirichlet type

An adaptation from our 5th order BFD scheme with periodic condition is required. As shown in [9], the scheme can be applied on the interval $(0, \pi)$, then a anti-symmetric reflection is performed onto the interval $(0, 2\pi)$. It has been proved in the same manuscript that the eigenvectors of the new problem are:

$$\begin{cases} \phi_k = \psi_k(\omega) - \psi_k(-\omega), \quad k = 1, 2 \\ \text{where} \\ \psi_k(\omega) = e^{i\omega x} + r_k e^{i\nu x} \\ \text{and} \\ \frac{1}{\sqrt{2\pi}} \sin(2Nx), \quad \frac{1}{\sqrt{2\pi}} \sin(Nx) \end{cases} \quad (39)$$

In order to get an approximation scheme for the end points of the interval $[0, \pi]$, we perform an extrapolation to the two additional ghost points needed, $x_{\frac{1}{4}} = -\frac{h}{4}$, $x_{-\frac{1}{4}} = -\frac{3h}{4}$ at the left boundary and $x_{(N+1)-\frac{1}{4}} = \pi + \frac{h}{4}$, $x_{(N+1)+\frac{1}{4}} = \pi + \frac{3h}{4}$ at the right one. As for the internal points for $1 \leq j \leq N$, the scheme remains the same.

The extrapolations are :

$$\begin{aligned} u_{-\frac{1}{4}} &= -u_{1+\frac{1}{4}} + 2g_0 + u_{xx}(0, t) \left(\frac{3h}{4}\right)^2 + \frac{1}{12} u_{xxxx}(0, t) \left(\frac{3h}{4}\right)^4 + O(h^6) \\ u_{\frac{1}{4}} &= -u_{1-\frac{1}{4}} + 2g_0 + u_{xx}(0, t) \left(\frac{h}{4}\right)^2 + \frac{1}{12} u_{xxxx}(0, t) \left(\frac{h}{4}\right)^4 + O(h^6) \end{aligned} \quad (40)$$

and

$$\begin{aligned} u_{(N+1)-\frac{1}{4}} &= -u_{N+\frac{1}{4}} + 2g_\pi + u_{xx}(\pi, t) \left(\frac{h}{4}\right)^2 + \frac{1}{12}u_{xxxx}(\pi, t) \left(\frac{h}{4}\right)^4 + O(h^6) \\ u_{(N+1)+\frac{1}{4}} &= -u_{N-\frac{1}{4}} + 2g_\pi + u_{xx}(\pi, t) \left(\frac{3h}{4}\right)^2 + \frac{1}{12}u_{xxxx}(\pi, t) \left(\frac{3h}{4}\right)^4 + O(h^6) \end{aligned} \quad (41)$$

where $u_{xx}(0, t), u_{xxxx}(0, t), u_{xx}(\pi, t), u_{xxxx}(\pi, t)$ can be computed from the PDE:

$$\begin{aligned} u_{xx}(0, t) &= u_t(0, t) - F(0, t) \\ u_{xx}(\pi, t) &= u_t(\pi, t) - F(\pi, t) \\ u_{xxxx}(0, t) &= u_{tt}(0, t) - F_t(0, t) - F_{xx}(0, t) \\ u_{xxxx}(\pi, t) &= u_{tt}(\pi, t) - F_t(\pi, t) - F_{xx}(\pi, t) \end{aligned} \quad (42)$$

The scheme at the nodes $x_{1-1/4}$ and $x_{1+1/4}$ becomes:

$$\begin{aligned} \frac{d^2}{dx^2}u_{1-\frac{1}{4}} &\approx \frac{1}{12(h/2)^2} \left[(30 - 8c)g_0 + (7 + 4c) \left(\frac{h}{4}\right)^2 u_{xx}(0, t) + \right. \\ &\quad \left. \frac{(-65 + 76c)}{12} \left(\frac{h}{4}\right)^4 u_{xxxx}(0, t) + \left(-46u_{1-\frac{1}{4}} + 17u_{1+\frac{1}{4}} - u_{1+\frac{3}{4}}\right) + \right. \\ &\quad \left. c \left(15u_{1-\frac{1}{4}} - 11u_{1+\frac{1}{4}} + 5u_{1+\frac{3}{4}} - u_{1+\frac{5}{4}}\right) \right] \end{aligned} \quad (43)$$

$$\begin{aligned} \frac{d^2}{dx^2}u_{1+\frac{1}{4}} &\approx \frac{1}{12(h/2)^2} \left[(-2 + 8c)g_0 + (-1 - 4c) \left(\frac{h}{4}\right)^2 u_{xx}(0, t) + \right. \\ &\quad \left. \frac{(-1 - 76c)}{12} \left(\frac{h}{4}\right)^4 u_{xxxx}(0, t) + \left(17u_{1-\frac{1}{4}} - 30u_{1+\frac{1}{4}} + 16u_{1+\frac{3}{4}} - u_{1+\frac{5}{4}}\right) + \right. \\ &\quad \left. c \left(-15u_{1-\frac{1}{4}} + 11u_{1+\frac{1}{4}} - 5u_{1+\frac{3}{4}} + u_{1+\frac{5}{4}}\right) \right] \end{aligned} \quad (44)$$

Similarly, the scheme at the nodes $x_{N-1/4}$ and $x_{N+1/4}$ is:

$$\begin{aligned} \frac{d^2}{dx^2}u_{N-\frac{1}{4}} &\approx \frac{1}{12(h/2)^2} \left[(-2 + 8c)g_\pi + (-1 - 4c) \left(\frac{h}{4}\right)^2 u_{xx}(\pi, t) + \right. \\ &\quad \left. \frac{(-1 - 76c)}{12} \left(\frac{h}{4}\right)^4 u_{xxxx}(\pi, t) + \left(-u_{N-\frac{5}{4}} + 16u_{N-\frac{3}{4}} - 30u_{N-\frac{1}{4}} + 17u_{N+\frac{1}{4}}\right) + \right. \\ &\quad \left. c \left(u_{N-\frac{5}{4}} - 5u_{N-\frac{3}{4}} + 11u_{N-\frac{1}{4}} - 15u_{N+\frac{1}{4}}\right) \right] \end{aligned} \quad (45)$$

$$\begin{aligned}
\frac{d^2}{dx^2}u_{N+\frac{1}{4}} \approx & \frac{1}{12(h/2)^2} \left[(30 - 8c)g_\pi + (7 + 4c) \left(\frac{h}{4}\right)^2 u_{xx}(\pi, t) + \right. \\
& \frac{(-65 + 76c)}{12} \left(\frac{h}{4}\right)^4 u_{xxxx}(\pi, t) + \left(-u_{N-\frac{3}{4}} + 17u_{N-\frac{1}{4}} - 46u_{N+\frac{1}{4}}\right) + \\
& \left. c \left(-u_{N-\frac{5}{4}} + 5u_{N-\frac{3}{4}} - 11u_{N-\frac{1}{4}} + 15u_{N+\frac{1}{4}}\right) \right] \quad (46)
\end{aligned}$$

The truncation errors at the boundaries are as follows:

$$\begin{aligned}
E(1 - \frac{1}{4}) &= -\frac{2359}{4423680}h^4u^{(6)} + c \left[-\frac{h^3}{96}u^{(5)} - \frac{3061}{1105920}h^4u^{(6)} \right] + O(h^5) \\
&= O(h^3)
\end{aligned}$$

$$\begin{aligned}
E(1 + \frac{1}{4}) &= -\frac{3071}{4423680}h^4u^{(6)} + c \left[\frac{h^3}{96}u^{(5)} - \frac{2699}{1105920}h^4u^{(6)} \right] + O(h^5) \\
&= O(h^3)
\end{aligned}$$

$$\begin{aligned}
E(N - \frac{1}{4}) &= -\frac{3071}{4423680}h^4u^{(6)} + c \left[-\frac{h^3}{96}u^{(5)} - \frac{2699}{1105920}h^4u^{(6)} \right] + O(h^5) \\
&= O(h^3)
\end{aligned}$$

$$\begin{aligned}
E(N + \frac{1}{4}) &= -\frac{2359}{4423680}h^4u^{(6)} + c \left[\frac{h^3}{96}u^{(5)} - \frac{3061}{1105920}h^4u^{(6)} \right] + O(h^5) \\
&= O(h^3)
\end{aligned}$$

We can see that the difference between the boundary and internal truncation errors (B.2) is of order 4.

2.3.2. Stability proof of the boundary scheme

As in the case of the periodic problem, it is necessary to show that the boundary operator $\Theta_{1/2}$ is non positive definite.

In order to do so, we first need to define the operator, in reference with the node $x = 0$.

In the first cell of the grid, the scheme is as follows:

$$\begin{bmatrix} u_{1-1/4} \\ u_{1+1/4} \end{bmatrix}_t = \left(A \begin{bmatrix} u_{1-1/4} \\ u_{1+1/4} \end{bmatrix} + B \begin{bmatrix} u_{1+3/4} \\ u_{1+5/4} \end{bmatrix} \right) \quad (47)$$

where:

$$A = \frac{1}{3h^2} \begin{bmatrix} -46 + 15c & 17 - 11c \\ 17 - 15c & -30 + 11c \end{bmatrix}, B = \frac{1}{3h^2} \begin{bmatrix} -1 + 5c & -c \\ 16 - 5c & -1 + c \end{bmatrix} \quad (48)$$

This gives us, similarly to the periodic boundary case, a possible solution for the unknowns:

$$\begin{aligned} C_1 &= \frac{7}{3}, & C_4 &= \frac{1}{2}, \\ D_1 &= -7 - C_2, & D_2 &= 0, \\ D_3 &= 0, & D_4 &= -C_2 - C_3 - \frac{17}{6}, \\ E_1 &= \frac{1}{18}(8c - 5), & E_4 &= \frac{1}{18}(-c - 1), \\ F_1 &= -\frac{47}{18} - C_2 - E_2 - \frac{4c}{9}, & F_2 &= 0, \\ F_3 &= 0, & F_4 &= \frac{1}{2}(-3 + c - 2C_2 - 2C_3 - 2E_2 - 2E_3) \end{aligned} \quad (49)$$

As for the second cell, the scheme is unchanged, but the stability is impacted by the scheme on the left side of the cell boundary $x = h$.

Stability condition on $x = 0$ and $x = h$ using boundary operators can be adapted in the following way.

The different operators are modified as follows:

$$\Theta_{1/2} =$$

$$\begin{bmatrix} u_{1-1/4} \\ u_{1+1/4} \end{bmatrix}^T M \begin{bmatrix} u_{1-1/4} \\ u_{1+1/4} \end{bmatrix} \quad (50)$$

where:

$$M = \frac{1}{12h}$$

$$\begin{bmatrix} M_{11} & M_{12} \\ M_{21} & M_{22} \end{bmatrix}$$

and

$$\begin{aligned} M_{11} &= -1 + 8c - 57C_2 - 48C_3 - 84E_2 - 48E_3 \\ M_{12} &= M_{21} = \frac{1}{3} (287 - 40c + 189C_2 + 144C_3 + 216C_3 + 144E_3) \\ M_{22} &= \frac{1}{3} (-319 + 56c - 171C_2 - 144C_3 - 180E_2 - 144E_3) \end{aligned}$$

In order to validate the stability condition of the scheme, we need to choose the rest of the unknowns in such a way that the operator $\Theta_{1/2}$ is non positive. The following solution fulfills the requirement:

$$C_2 = -7, C_3 = 0, E_2 = 0, E_3 = \frac{25}{3} + \frac{c}{6}.$$

Finally, it remains to verify if the boundary operator $\Theta_{3/2}$ related to the next node $x_2 = h$ is non positive as well under those conditions:

$$\Theta_{3/2} =$$

$$\begin{bmatrix} u_{j-5/4} \\ u_{j-3/4} \\ u_{j-1/4} \\ u_{j+1/4} \end{bmatrix}^T M \begin{bmatrix} u_{j-5/4} \\ u_{j-3/4} \\ u_{j-1/4} \\ u_{j+1/4} \end{bmatrix} \quad (51)$$

where:

$$M = \frac{1}{36h} \begin{bmatrix} -93 - 8c & 143 + 24c & -7 - 40c & -43 + 24c \\ 143 + 24c & -277 - 40c & 125 + 56c & 9 - 40c \\ -7 - 40c & 125 + 56c & -373 - 40c & 3(85 + 8c) \\ -43 + 24c & 9 - 40c & 3(85 + 8c) & -221 - 8c \end{bmatrix}$$

Indeed, it can be shown that for all values $-1 < c < 1$, all eigenvalues of the last M matrix are non positive.

2.3.3. Numerical Results

Our theory on stability and order of convergence is confirmed by numerical results (see Figure 1). We used the approximation (43) to solve the heat problem (55) on the interval $[0, 1]$ where $F(x, t)$ and the initial condition were chosen such that the exact solution is $u(x, t) = \exp(\cos(x - t))$. The scheme was run with $N = 24, 36, 48, 72, 84$ and 4th Order Explicit Runge-Kutta was used for time integration.

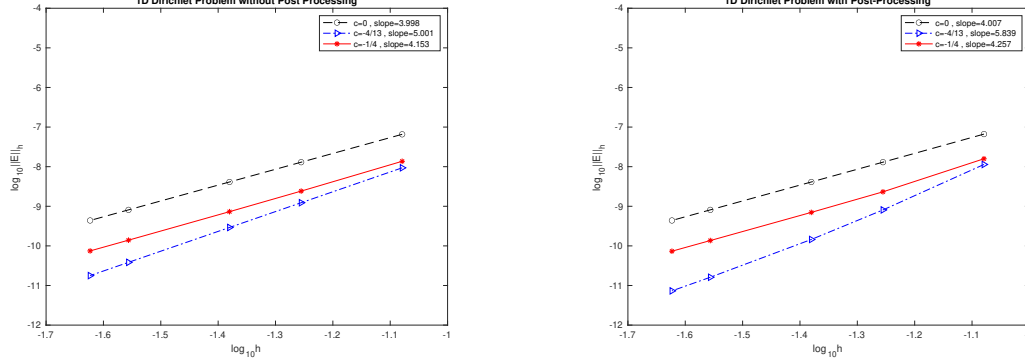


Figure 1: Error and Convergence plots, $\log_{10}\|\mathbf{E}\|$ vs. $\log_{10} h$ for 1D scheme - Dirichlet boundary conditions

2.4. Conclusion

We combined the advantages of viewing our BFD scheme first as a FE type and secondly as a FD type. This allowed us to provide a proof of stability in an easy manner based on the standard tools developed for DG methods, and then the optimal rate of convergence was proved through the tools developed for BFD methods.

2.5. Generalization to Two dimensions

The generalization to two dimensions is rather straightforward, as the two-dimensional scheme is constructed as a tensor product of the one-dimensional scheme, presented in the previous subsection.

Let us first consider the following problem with periodic boundary conditions:

$$\begin{cases} \frac{\partial u}{\partial t}(x, y, t) = \frac{\partial^2}{\partial x^2}u(x, y, t) + \frac{\partial^2}{\partial y^2}u(x, y, t) + F(x, y, t), \\ u(t=0) = f(x, y) \end{cases} \quad (x, y) \in (0, 2\pi) \times (0, 2\pi), \quad t \geq 0 \quad (52)$$

2.5.1. Proof of Optimal Convergence

Let us present the two-dimensional 5th order approximation of four-point block. Let us consider the following grid. In each cell whose center is located

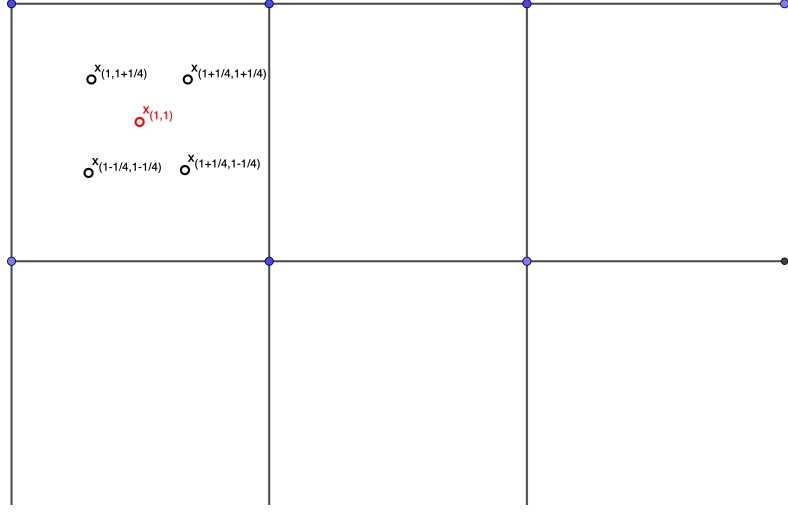


Figure 2: Grid in 2 Dimensions - Illustration

in $x_{(i,j)}$, we define four nodes as illustrated in Figure 2:

$$\begin{aligned}
 x_{(i-1/4,j-1/4)} &= x_j + \left(-\frac{h}{4}, -\frac{h}{4}\right) \\
 x_{(i+1/4,j+1/4)} &= x_j + \left(\frac{h}{4}, \frac{h}{4}\right) \\
 x_{(i+1/4,j-1/4)} &= x_j + \left(\frac{h}{4}, -\frac{h}{4}\right) \\
 x_{(i-1/4,j+1/4)} &= x_j + \left(-\frac{h}{4}, \frac{h}{4}\right) \\
 h &= 2\pi/N, \quad i, j = 1, \dots, N
 \end{aligned} \tag{53}$$

where

$$x_{(i,j)} = \left(h(i-1) + \frac{h}{2}, h(j-1) + \frac{h}{2}\right) \tag{54}$$

Altogether there are $4N^2$ points on the grid, with a distance of $h/2$ between them when located at the same x or y coordinate.

2.5.2. Proof of Stability

The generalization to higher dimensions is done seamlessly. Indeed, the operator $\Theta_{j-1/2}$ as defined in the previous section for one dimension only, can be defined for two dimensions. In two dimensions, it is a combination of the contributions from each side of the cell and the average of two integrals of one dimension, in the x and y direction respectively. Since all contributions are non positive, as shown in the one dimensional case, the combination of those is non-positive as well.

2.5.3. Numerical Results

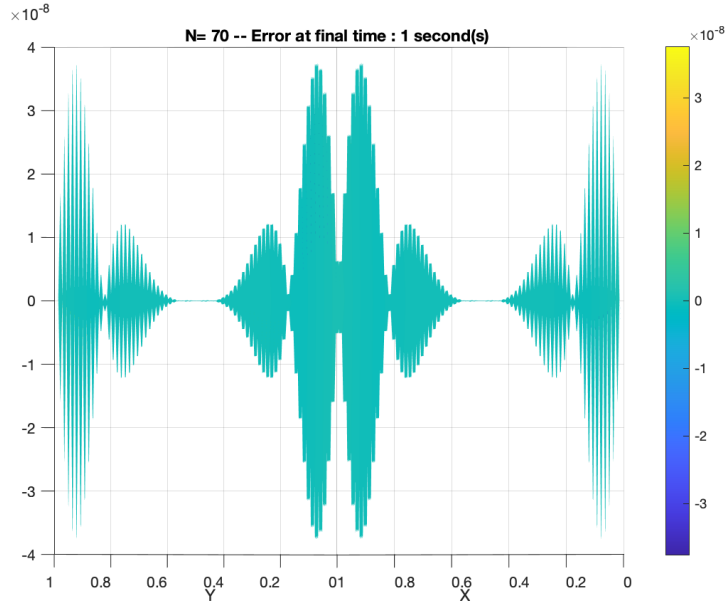


Figure 3: Error plots for 2D Periodic scheme, $N=70$

Our theory on stability and order of convergence is demonstrated by numerical results (see Figure 3). The scheme was run for $u(x, t) = \exp(\cos(2\pi(x + y - t)))$ on the interval $[0, 1] \times [0, 1]$ and $N = 50, 60, 70, 80$ with a 4th order explicit Runge-Kutta time propagator and final time $t = 1$. In Figure 4, the convergence plots appear with $c = 0, -1/4, -4/13$ and the optimal convergence rate is reached for $c = -4/13$, a 6th order with post-processing.

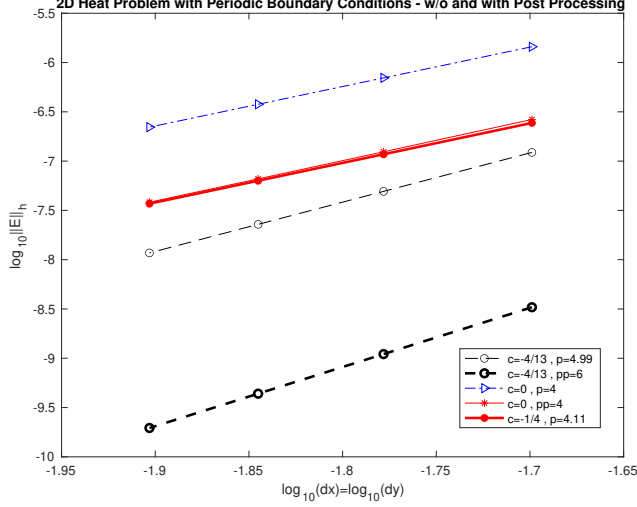


Figure 4: Error and Convergence plots, $\log_{10}\|\mathbf{E}\|$ vs. $\log_{10} dx = dy$ for 2D Periodic scheme

2.5.4. Non-Periodic Boundary Conditions

Let us first consider the following problem with non-periodic boundary conditions:

$$\left\{ \begin{array}{l} \frac{\partial u}{\partial t}(x, y, t) = \frac{\partial^2}{\partial x^2}u(x, y, t) + \frac{\partial^2}{\partial y^2}u(x, y, t) + F(x, y, t) , \\ \quad \quad \quad (x, y) \in (0, \pi) \times (0, \pi) , t \geq 0 \\ u(t = 0) = f(x, y) \\ u(0, y, t) = g_0(y, t) \\ u(\pi, y, t) = g_\pi(y, t) \\ u(x, 0, t) = h_0(x, t) \\ u(x, \pi, t) = h_\pi(x, t) \end{array} \right. \quad (55)$$

In order to get an approximation scheme for the boundary points of the rectangle $[0, \pi] \times [0, \pi]$, we perform an extrapolation for the additional ghost points needed as illustrated in Figure 5.

In the x-axis direction: $x_{(\frac{1}{4}, i)} = (-\frac{h}{4}, y_i)$, $x_{(-\frac{1}{4}, i)} = (-\frac{3h}{4}, y_i)$ on one end and $x_{((N+1)-\frac{1}{4}, i)} = (\pi + \frac{h}{4}, y_i)$, $x_{((N+1)+\frac{1}{4}, i)} = (\pi + \frac{3h}{4}, y_i)$ on the other end. As for the internal points $x_{i,j}$, $1 \leq i, j \leq N$, the scheme remains the same.

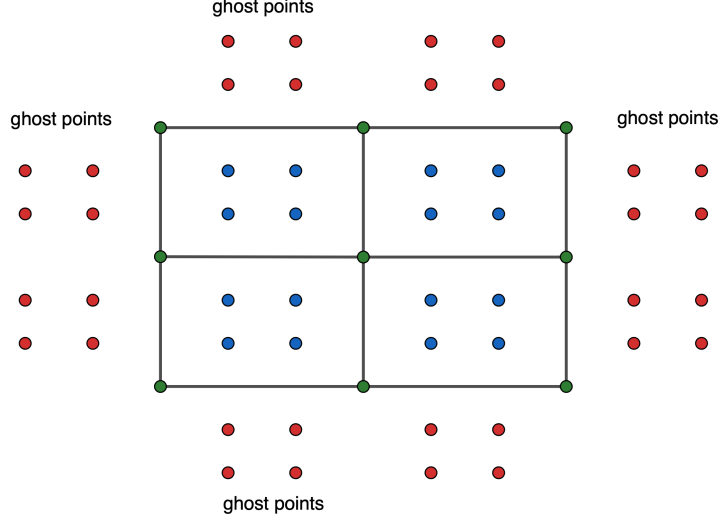


Figure 5: Grid and Ghost Points in 2D - Illustration

It follows that:

$$\begin{aligned}
 u_{(-\frac{1}{4},i)} &= -u_{(1+\frac{1}{4},i)} + 2g_0(y_i, t) + u_{xx}(0, y_i, t) \left(\frac{3h}{4}\right)^2 + \\
 &\quad \frac{1}{12}u_{xxxx}(0, y_i, t) \left(\frac{3h}{4}\right)^4 + O(h^6) \\
 u_{(\frac{1}{4},i)} &= -u_{(1-\frac{1}{4},i)} + 2g_0(y_i, t) + u_{xx}(0, y_i, t) \left(\frac{h}{4}\right)^2 + \\
 &\quad \frac{1}{12}u_{xxxx}(0, y_i, t) \left(\frac{h}{4}\right)^4 + O(h^6)
 \end{aligned} \tag{56}$$

Similarly:

$$\begin{aligned}
 u_{((N+1)-\frac{1}{4},i)} &= -u_{(N+\frac{1}{4},i)} + 2g_\pi(y_i, t) + u_{xx}(\pi, y_i, t) \left(\frac{h}{4}\right)^2 + \\
 &\quad \frac{1}{12}u_{xxxx}(\pi, y_i, t) \left(\frac{h}{4}\right)^4 + O(h^6) \\
 u_{((N+1)+\frac{1}{4},i)} &= -u_{(N-\frac{1}{4},i)} + 2g_\pi(y_i, t) + u_{xx}(\pi, y_i, t) \left(\frac{3h}{4}\right)^2 + \\
 &\quad \frac{1}{12}u_{xxxx}(\pi, y_i, t) \left(\frac{3h}{4}\right)^4 + O(h^6)
 \end{aligned} \tag{57}$$

where $u_{xx}(0, y_i, t), u_{xxxx}(0, t), u_{xx}(\pi, y_i, t), u_{xxxx}(\pi, y_i, t)$ can be computed from the PDE:

$$\begin{aligned}
u_{xx}(0, y, t) &= u_t(0, y, t) - u_{yy}(0, y, t) - F(0, y, t) \\
u_{xx}(\pi, y, t) &= u_t(\pi, y, t) - u_{yy}(\pi, y, t) - F(\pi, y, t) \\
u_{xxxx}(0, y, t) &= u_{tt}(0, y, t) - 2u_{tyy}(0, y, t) - F_t(0, y, t) + \\
&\quad u_{yyyy}(0, y, t) + F_{yy}(0, y, t) - F_{xx}(0, y, t) \\
u_{xxxx}(\pi, y, t) &= u_{tt}(\pi, y, t) - 2u_{tyy}(\pi, y, t) - F_t(\pi, y, t) + \\
&\quad u_{yyyy}(\pi, y, t) + F_{yy}(\pi, y, t) - F_{xx}(\pi, y, t)
\end{aligned} \tag{58}$$

For the y -axis direction, the extrapolations are analogous.

2.5.5. Numerical Results

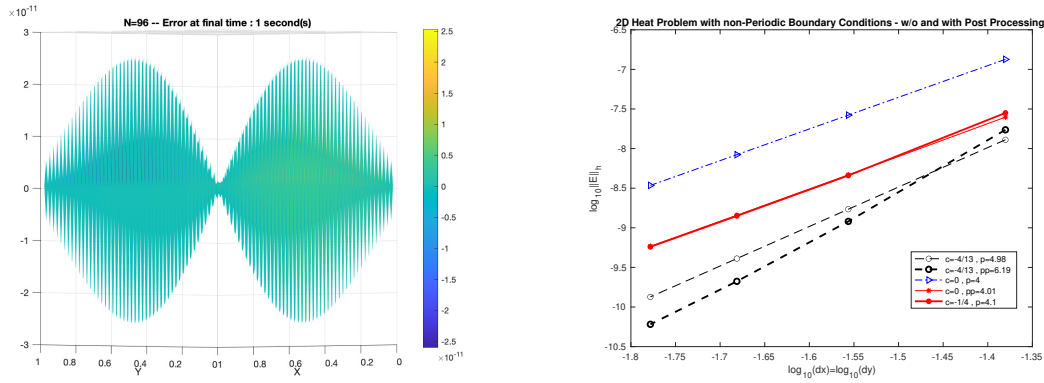


Figure 6: Error and Convergence plots, $\log_{10}||\mathbf{E}||$ vs. $\log_{10} h$ for 2D scheme Dirichlet boundary conditions

Our theory on stability and order of convergence is demonstrated by numerical results (see Figure 6). The scheme was run for $u(x, t) = \exp(\cos(x + y - t))$ on the interval $[0, 1] \times [0, 1]$ and $N = 24, 36, 48, 60$ with a 4th order explicit Runge-Kutta time propagator and final time $t = 1$. In Figure 6, the convergence plots appear with $c = 0, -1/4, -4/13$ and the optimal convergence rate is reached for $c = -4/13$, a 6th order with post-processing.

3. Future Work

The schemes that we constructed and analyzed in this manuscript are defined in rectangular domains. Our project's next stage is to derive block finite difference schemes to solve the heat equation in two and three-dimensional, complicated geometries.

We also intend to derive block finite difference schemes to solve the advection equation and hyperbolic systems.

References

- [1] C.-W. Shu B. Cockburn, M. Luskin and E. Süli. Enhanced accuracy by post-processing for finite element methods for hyperbolic equations. *Mathematics of Computation*, (72):577–606, 2003.
- [2] I. Babuska, C.E. Baumann, and J.T. Oden. A discontinuous hp finite element method for diffusion problems: 1-d analysis. *Computers & Mathematics with Applications*, 37(9):103 – 122, 1999.
- [3] SC. E. Baumann and J. T. Oden. A discontinuous hp finite element method for convection-diffusion problems. *Comput. Methods Appl. Mech. Engrg.*, (175):311–341, 1999.
- [4] Susanne C. Brenner and L. Ridgway Scott. *The Mathematical theory of finite element methods*, volume 46. Springer, New York, 2003.
- [5] Bernardo Cockburn and Chi-Wang Shu. Runge–kutta discontinuous galerkin methods for convection-dominated problems. *J. Sci. Comput.*, (16(3)):173–261, 2001.
- [6] R. Courant, K. Friedrichs, and H. Lewy. Über die partiellen Differenzengleichungen der mathematischen Physik. *Mathematische Annalen*, 100:32–74, 1928.
- [7] A. Ditkowski. *High Order Finite Difference Schemes for the Heat Equation Whose Convergence Rates are Higher Than Their Truncation Errors*, pages 167–178. Springer International Publishing, Cham, 2015.
- [8] A. Ditkowski and S. Gottlieb. Error inhibiting block one-step schemes for ordinary differential equations. *Journal of Scientific Computing*, Apr 2017.
- [9] Paz Fink. Error Inhibiting Schemes for Initial Boundary Value Heat Equation. <https://arxiv.org/abs/2010.00476>.
- [10] Bertil Gustafsson, Heinz-Otto Kreiss, and Joseph Oliger. *Time dependent problems and difference methods*, volume 24. John Wiley & Sons, 1995.

- [11] Thomas J.R. Hughes. *The Finite Element Method*. Dover Publications, Inc., 2007.
- [12] H. Atkins J. Ryan, C.-W. Shu. Extension of a post processing technique for the discontinuous galerkin method for hyperbolic equations with application to an aeroacoustic problem. *J. Sci. Comput.*, (26(3)):821–843, 2005.
- [13] H.-O. Kreiss, Manteuffel T.A., B. Swartz, B. Wendroff, and Jr. A.B. White. Supra-convergent schemes on irregular grids. *Mathematics of Computation*, 47:537 – 554, 1986.
- [14] Peter D Lax and Robert D Richtmyer. Survey of the stability of linear finite difference equations. *Communications on pure and applied mathematics*, 9(2):267–293, 1956.
- [15] K. W. Morton and D. F. Mayers. *Numerical Solution of Partial Differential Equations: An Introduction*. Cambridge University Press, New York, NY, USA, 2005.
- [16] Chi-Wang Shu. Discontinuous galerkin methods: general approach and stability. *Numerical solutions of partial differential equations*, 201, 2009.
- [17] Gilbert Strang and George Fix. *An Analysis of the Finite Element Method*. Wellesley-Cambridge Press, 2008.
- [18] James J. Sylvester. A demonstration of the theorem that every homogeneous quadratic polynomial is reducible by real orthogonal substitutions to the form of a sum of positive and negative squares. *Philosophical Magazine Series*, 4(23):138–142, 1852.
- [19] Mengping Zhang and Chi-Wang Shu. An analysis of three different formulations of the discontinuous galerkin method for diffusion equations. *Mathematical Models and Methods in Applied Sciences*, 13(03):395–413, 2003.

Appendix A. Proof of Optimal Convergence

In this section, the tools developed in [7] and [9] will be used, exploiting the fact that our scheme is of FD type.

We will perform a Fourier like analysis for this purpose.

Since Q , the FD discrete operator, is not diagonalizable by standard Fourier transform, we split the Fourier spectrum into low and high frequencies as follows: Let $\omega \in \{-N/2, \dots, N/2\}$ and

$$\nu = \begin{cases} \omega - N & \omega > 0 \\ \omega + N & \omega < 0 \end{cases} \quad (\text{A.1})$$

Then, for $\omega > 0$:

$$e^{i\omega x_{j-1/4}} = i e^{i\nu x_{j-1/4}} \quad \text{and} \quad e^{i\omega x_{j+1/4}} = -i e^{i\nu x_{j+1/4}}. \quad (\text{A.2})$$

We note that a similar analysis can be performed for $\omega < 0$.

We denote the vectors $e^{i\omega \mathbf{x}}$ and $e^{i\nu \mathbf{x}}$ by:

$$e^{i\omega \mathbf{x}} = \begin{pmatrix} \vdots \\ e^{i\omega x_{j-1/4}} \\ e^{i\omega x_{j+1/4}} \\ \vdots \end{pmatrix}, \quad e^{i\nu \mathbf{x}} = \begin{pmatrix} \vdots \\ e^{i\nu x_{j-1/4}} \\ e^{i\nu x_{j+1/4}} \\ \vdots \end{pmatrix} \quad (\text{A.3})$$

We look for eigenvectors in the form of:

$$\psi_k(\omega) = \alpha_k \frac{e^{i\omega \mathbf{x}}}{\sqrt{2\pi}} + \beta_k \frac{e^{i\nu \mathbf{x}}}{\sqrt{2\pi}} \quad (\text{A.4})$$

where, for normalization, it is required that $|\alpha_k|^2 + |\beta_k|^2 = 1$, $k = 1, 2$.

Let us note that each component of the linear combination $e^{i\omega \mathbf{x}}$ and $e^{i\nu \mathbf{x}}$ is not an eigenvector in the classical sense, since only the linear combination verifies the initial condition.

It follows that :

$$Q e^{i\omega \mathbf{x}} = \text{diag}(\mu_1, \mu_2, \dots, \mu_1, \mu_2) e^{i\omega \mathbf{x}} \quad (\text{A.5})$$

$$Q e^{i\nu \mathbf{x}} = \text{diag}(\sigma_1, \sigma_2, \dots, \sigma_1, \sigma_2) e^{i\nu \mathbf{x}} \quad (\text{A.6})$$

where:

$$\begin{aligned} \mu_1 = \frac{1}{3h^2} & \left[(32 - 15c) \cos\left(\frac{h\omega}{2}\right) + (6c - 2) \cos(h\omega) - \right. \\ & \left. c \left(\cos\left(\frac{3h\omega}{2}\right) + 32i \sin^5\left(\frac{h\omega}{4}\right) \cos\left(\frac{h\omega}{4}\right) \right) + 10c - 30 \right] \end{aligned}$$

$$\begin{aligned}\mu_2 = & \frac{1}{3h^2} \left[(32 - 15c) \cos\left(\frac{h\omega}{2}\right) - c \cos\left(\frac{3h\omega}{2}\right) + \right. \\ & \left. (6c - 2) \cos(h\omega) + 32ic \sin^5\left(\frac{h\omega}{4}\right) \cos\left(\frac{h\omega}{4}\right) + 10c - 30 \right]\end{aligned}$$

$$\begin{aligned}\sigma_1 = & \frac{1}{3h^2} \left[(15c - 32) \cos\left(\frac{h\omega}{2}\right) + c \cos\left(\frac{3h\omega}{2}\right) + \right. \\ & \left. (6c - 2) \cos(h\omega) + 32ic \sin\left(\frac{h\omega}{4}\right) \cos^5\left(\frac{h\omega}{4}\right) + 10c - 30 \right]\end{aligned}$$

$$\begin{aligned}\sigma_2 = & \frac{1}{3h^2} \left[(15c - 32) \cos\left(\frac{h\omega}{2}\right) + c \cos\left(\frac{3h\omega}{2}\right) + \right. \\ & \left. (6c - 2) \cos(h\omega) - 32ic \sin\left(\frac{h\omega}{4}\right) \cos^5\left(\frac{h\omega}{4}\right) + 10c - 30 \right]\end{aligned}$$

In order to find the coefficients α_k, β_k and the eigenvalues (symbols) \hat{Q}_k for $\omega \neq 0$, we look at some node x_j and solve the following system of equations:

$$\begin{aligned}\mu_1 \frac{\alpha_k}{\sqrt{2\pi}} e^{i\omega x_{j-\frac{1}{4}}} + \sigma_1 \frac{\beta_k}{\sqrt{2\pi}} e^{i\nu x_{j-\frac{1}{4}}} &= \hat{Q}_k \left(\frac{\alpha_k}{\sqrt{2\pi}} e^{i\omega x_{j-\frac{1}{4}}} + \frac{\beta_k}{\sqrt{2\pi}} e^{i\nu x_{j-\frac{1}{4}}} \right) \\ \mu_2 \frac{\alpha_k}{\sqrt{2\pi}} e^{i\omega x_{j+\frac{1}{4}}} + \sigma_2 \frac{\beta_k}{\sqrt{2\pi}} e^{i\nu x_{j+\frac{1}{4}}} &= \hat{Q}_k \left(\frac{\alpha_k}{\sqrt{2\pi}} e^{i\omega x_{j+\frac{1}{4}}} + \frac{\beta_k}{\sqrt{2\pi}} e^{i\nu x_{j+\frac{1}{4}}} \right)\end{aligned} \quad (\text{A.7})$$

We denote $r_k = i \frac{\beta_k}{\alpha_k}$ and use Eq. (A.2) to obtain a simpler system:

$$\begin{aligned}\mu_1 - \sigma_1 r_k &= \hat{Q}_k (1 - r_k) \\ \mu_2 + \sigma_2 r_k &= \hat{Q}_k (1 + r_k)\end{aligned} \quad (\text{A.8})$$

Thus, the expressions for r_k and the eigenvalues (symbols) \hat{Q}_k are:

$$\begin{aligned}r_1 &= (\Omega + \Delta) i \\ r_2 &= (\Omega - \Delta) i\end{aligned} \quad (\text{A.9})$$

where

$$\Omega = \frac{2 \cos\left(\frac{\omega h}{2}\right) (-16 + 7c + c \cos(\omega h))}{32c \sin\left(\frac{\omega h}{4}\right) \cos\left(\frac{\omega h}{4}\right)^5} \quad (\text{A.10})$$

$$\text{and} \quad (\text{A.11})$$

$$\Delta = \sqrt{2} [4(3c - 8)(5c - 8) \cos(h\omega) + c(9c - 16) \cos(2h\omega) + c(59c - 240) + 256]^{\frac{1}{2}} \quad (\text{A.12})$$

$$\hat{Q}_1(\omega) = \frac{(6c - 2) \cos(h\omega) + 10c - 30 + \Delta}{3h^2}, \quad (\text{A.13})$$

$$\hat{Q}_2(\omega) = \frac{(6c - 2) \cos(h\omega) + 10c - 30 - \Delta}{3h^2}$$

Using the normalization condition $|\alpha_k|^2 + |\beta_k|^2 = 1$, $k = 1, 2$, we choose the coefficients α_k, β_k to be:

$$\alpha_1 = \frac{1}{\sqrt{1 + |r_1|^2}}, \quad \beta_1 = -i \frac{r_1}{\sqrt{1 + |r_1|^2}} \quad (\text{A.14})$$

$$\alpha_2 = \frac{|r_2|/r_2}{\sqrt{1 + |r_2|^2}}, \quad \beta_2 = -i \frac{|r_2|}{\sqrt{1 + |r_2|^2}} \quad (\text{A.15})$$

For $\omega h \ll 1$ the eigenvalues are:

$$\hat{Q}_1(\omega) = -\omega^2 - \frac{(4 + 13c)\omega^6 h^4}{2880(-2 + c)} + O(h^6) \quad (\text{A.16})$$

and

$$\hat{Q}_2(\omega) = \frac{32(-2 + c)}{3h^2} - \frac{(-5 + 6c)\omega^2}{3} + \frac{(-1 + 3c)\omega^4 h^2}{18} + O(h^4) \quad (\text{A.17})$$

If the initial condition is

$$\mathbf{v}_{j-\frac{1}{4}}(0) = e^{i\omega x_{j-\frac{1}{4}}}, \quad \mathbf{v}_{j+\frac{1}{4}}(0) = e^{i\omega x_{j+\frac{1}{4}}} ; \quad \omega^2 h \ll 1 \quad (\text{A.18})$$

Then

$$\begin{aligned} \mathbf{v}_{j-\frac{1}{4}}(t) = & \left(e^{-\omega t^2} \left[1 - \frac{(4+13c)\omega^6 t h^4}{1024(-2+c)} \right] + O(h^6) \right) e^{i\omega x_{j-\frac{1}{4}}} + \\ & \left(\frac{ic(\omega h)^5}{1024(-2+c)} + O(h^6) \right) e^{i\nu x_{j-\frac{1}{4}}} \end{aligned} \quad (\text{A.19})$$

The same expression hold for $x_{j+1/4}$. Therefore the scheme is of 4th order in general, and it is of 5th order if $c = -4/13$.

Appendix B. Derivation of the Scheme

In order to build the BFD scheme, (18), we start with imposing the conditions for obtaining a 3rd order truncation error, using Taylor's expansions to get:

$$\begin{aligned} \frac{d^2}{dx^2} u_{j-1/4} & \approx \frac{1}{12(h/2)^2} \left[\left(-u_{j-\frac{5}{4}} + 16u_{j-\frac{3}{4}} - 30u_{j-\frac{1}{4}} + 16u_{j+\frac{1}{4}} - u_{j+\frac{3}{4}} \right) + \right. \\ & \quad \left. c_1 \left(u_{j-\frac{5}{4}} - 5u_{j-\frac{3}{4}} + 10u_{j-\frac{1}{4}} - 10u_{j+\frac{1}{4}} + 5u_{j+\frac{3}{4}} - u_{j+\frac{5}{4}} \right) \right] \\ \frac{d^2}{dx^2} u_{j+1/4} & \approx \frac{1}{12(h/2)^2} \left[\left(-u_{j-\frac{3}{4}} + 16u_{j-\frac{1}{4}} - 30u_{j+\frac{1}{4}} + 16u_{j+\frac{3}{4}} - u_{j+\frac{5}{4}} \right) - \right. \\ & \quad \left. c_2 \left(u_{j-\frac{5}{4}} - 5u_{j-\frac{3}{4}} + 10u_{j-\frac{1}{4}} - 10u_{j+\frac{1}{4}} + 5u_{j+\frac{3}{4}} - u_{j+\frac{5}{4}} \right) \right] \end{aligned} \quad (\text{B.1})$$

Due to symmetry considerations, we will further require that $c_1 = c_2 = c$ hence the truncation error of the scheme will be:

$$\begin{aligned} T_e(j - \frac{1}{4}) & = \left[-\frac{h^4}{1440} u^{(6)} - c \left[\frac{h^3}{96} u^{(5)} + \frac{h^4}{384} u^{(6)} \right] + O(h^5) \right]_{x_{j-1/4}} = O(h^3) \\ T_e(j + \frac{1}{4}) & = \left[-\frac{h^4}{1440} u^{(6)} - c \left[-\frac{h^3}{96} u^{(5)} + \frac{h^4}{384} u^{(6)} \right] + O(h^5) \right]_{x_{j+1/4}} = O(h^3) \end{aligned} \quad (\text{B.2})$$

The motivation leading to this scheme is that the highly oscillating $O(h^3)$ terms will be dissipated, while the $O(h^4)$ terms will cancel each other for a proper value of c .

From a naive analysis, we could assume that the optimal c is $-4/15$, a conclusion which will be proven wrong in our further analysis.

This is confirmed by the following numerical results.

Appendix B.0.1. Numerical Results

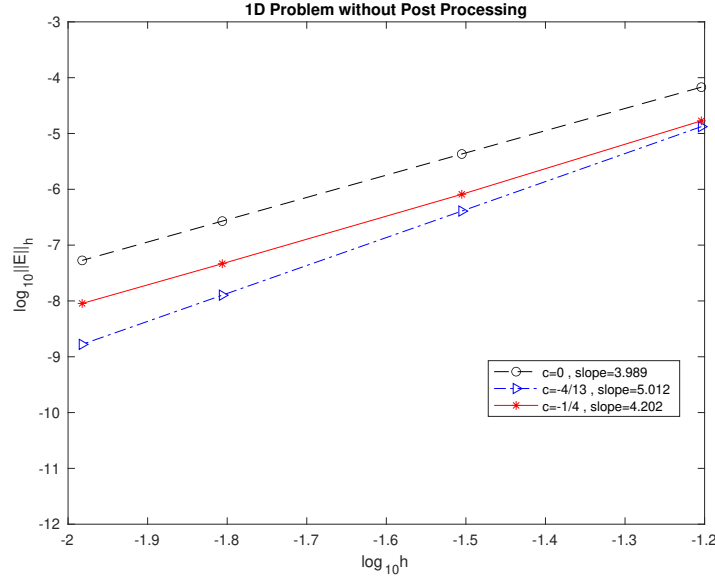


Figure B.7: Convergence plots, $\log_{10}\|E\|$ vs. $\log_{10} h$, Scheme (18) without post-processing

The scheme was run for $u(x, t) = \exp(\cos(2\pi(x - t)))$ on the interval $[0, 1]$ and $N = 16, 32, 64, 96$ with a 6th order implicit Gauss-Legendre time propagator and final time $t = 1$. In Figure B.7, the convergence plots appear with $c = 0, -1/4, -4/13$ and the optimal convergence rate is reached for $c = -4/13$, a 6th order with post-processing (see Figure B.8). Details of the post-processing procedure are provided in Appendix C.

Appendix C. Post-processing

Appendix C.1. Post-Processing - Heat problem with Periodic Boundary Conditions

The post-processing procedure is based on the fact that the global error is highly oscillatory. A filter is then applied on the high mode, thus gaining

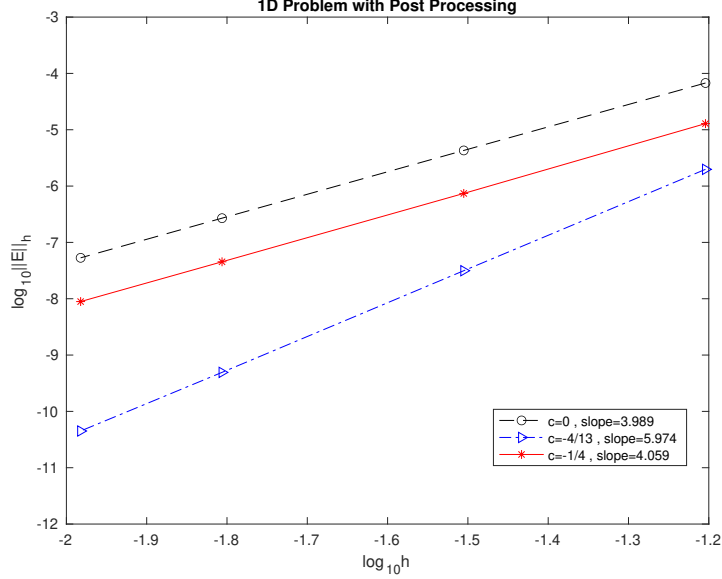


Figure B.8: Convergence plots, $\log_{10}\|\mathbf{E}\|$ vs. $\log_{10} h$, Scheme (18) with post-processing

an order of convergence.

Appendix C.2. Post-Processing for Non-periodic boundary conditions of Dirichlet type

For non periodic conditions, the error is not located in high modes only, hence a different technique is applied.

Every 12 grid points, we perform an approximation to obtain a 6th order polynomial. We then compute the related approximation for the batch of points. In two dimensions, we scanned the grid in the x-direction, approximated, and then scanned the y-direction using the previously obtained approximation.

Both of the algorithms were adapted based on the enhancing process originally designed for hyperbolic equations by [1],[12].